The Effects of Carbon, Boron and Vanadium on the Microstructural Evolution and Hardness of Steel-based Hardfacing Alloys

Kyle Rafa

California Polytechnic State University

Materials Engineering Senior Project

Advisor: Dr. Blair London

Corporate Sponsor: Scoperta Inc.

June 4, 2010

Approval Page

Project Title: The Effects of Carbon, Boron and Vanadium on the Microstructural Evolution and Hardness of Steel-based Hardfacing Alloys

Author: Kyle Rafa

Date Submitted: June 4, 2010

CAL POLY STATE UNIVERSITY
Materials Engineering Department

Since this project is a result of a class assignment, it has been graded and accepted as fulfillment of the course requirements. Acceptance does not imply technical accuracy or reliability. Any use of information in this report is done at the risk of the user. These risks may include catastrophic failure of the device or infringement of patent or copyright laws. The students and staff of Cal Poly State University, San Luis Obispo cannot be held liable for any misuse of the project.

Prof. Blair London _____
Faculty Advisor Signature

Prof. Trevor Harding _____
Department Chair Signature

Aknowledgements

I would like to thank my corporate sponsor Scoperta Inc. and specifically Justin Cheney and John Madok for providing samples as well as technical expertise in the field of hardfacing. My advisor Dr. Blair London provided me with support and insight without which I would likely have lost my way early on. Dr. Dan Walsh helped support my findings utilizing his expertise in the field of welding solidification and phase nucleation. Finally, I would like to thank all of Dr. Blair London's Senior Project group for providing a sounding board for my ideas and collectively applying their knowledge of metals towards various aspects of my project.

Abstract

Current hardfacing alloys provide insufficient wear resistance due to either cracking or significant material wear. To increase wear resistance of steel-based hardfacing alloys, the effects of composition on microstructure and hardness were investigated in a progression of alloys. Initially, seven new alloys were prepared varying the carbon-boron ratio with the total constant at 3 wt%. Small arc-melt cast circular ingots were produced roughly 1 x 0.5 inches. Metallography provided insufficient phase magnification, thus a SEM equipped with EDS was used, allowing for microstructure and phase composition analysis. Four distinct carbide phases were found and image analysis software allowed for carbide volume fraction measurements. It was determined that the sample consisting of 0.5 wt% carbon produced the most promising microstructure with a large volume fraction of NbC and $M_{23}(C,B)_6$ distributed in a continuous ferrite matrix. The 0.5 wt% C sample resulted in a hardness of 950 HV which exceeded the minimum 830 HV previous studies have shown to provide adequate wear resistance. XRD analysis alone produced inconclusive results, however by comparison to EDS compositions, phase stoichiometries were determined. A second round of new alloys was tested holding the composition similar to the 0.5 wt% C sample where vanadium was incrementally substituted for tungsten. These alloys demonstrated a reduced carbide volume fraction further supported with microhardness showing a reduction in the average hardness of 200 HV compared to the first round alloys. This suggests that the 0.5 wt% carbon sample shows the highest likelihood of increased wear resistance of the alloys tested. Overall, increasing the carbon content produced a $M_{2,3}C$ which in previous studies has been shown to be detrimental to the wear resistance of steel.

Keywords: Hardfacing, Alloy Development, Carbides, Wear Resistance, Microstructural Progression

Table of Contents

List of Figures

List of Tables

Introduction

I. Problem Statement

Hardfacing alloys are commonly used in many applications including front loader shovels used in ore mining. Current hardfacing alloys produced by Scoperta provide insufficient wear resistance due to either material loss or cracking of the alloy upon weld depositing. The goal of this study is to gain understanding into how carbon, boron, and vanadium effect the volume fraction and morphology of various microstructural constituents, ultimately leading to a high wear resistance. Utilizing the SEM and XRD, various alloy microstructures will be analyzed and promising alloys will show a large volume fraction of carbides distributed in a continuously connected ferrite matrix.

II. What is Hardfacing?

Hardfacing is a process by which a sacrificial layer is welded onto a structural component to prolong the part life (Figure 1).

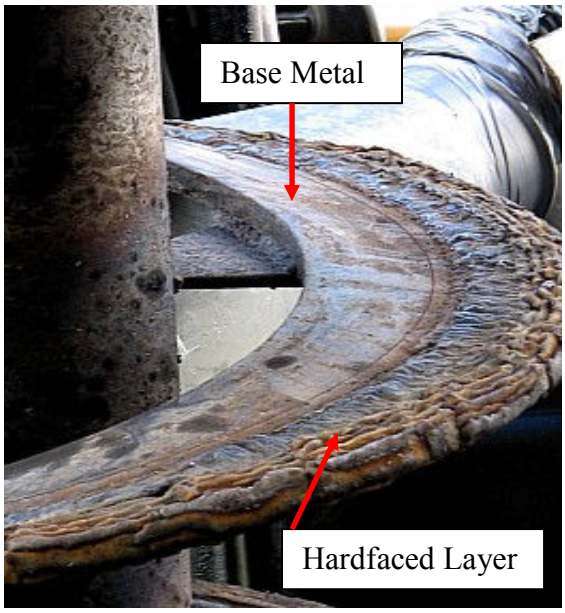

Figure 1- A hardfaced corkscrew used in mixing cement[1].

In environments where critical structural components are exposed to harsh wear environments, sacrificial layers are deposited through various methods including metal-inert gas welding and twin-wire arc spray. Once a layer has been deposited, it wears preferentially at a slower rate than the structural component, prolonging the part's life.

III. Carbides and Their Effect on Wear

Due to their ceramic nature, carbides themselves are hard and brittle. Carbides have good abrasive wear resistance, however this is overshadowed by a high notch sensitivity. If a carbide were used by itself as a sacrificial layer, surface defects would provide localized stress concentrations amplifying the applied load causing fracture. Continued fracture would cause the carbide layer to crumble quickly exposing the critical structural component. This is reduced by forming carbides in a ductile matrix. The matrix has a high toughness with the ability to prevent crack growth. The carbides provide wear resistance and act to shield the matrix from abrasion while the matrix prevents stress concentrations around the carbides. However, in steel, the size and distribution of carbides controls the wear resistance[2]. Consider a fixed volume of any carbide. If this volume is concentrated at only one localized region, it becomes easy for an abrasive to wear the matrix surrounding the carbide. However, if the same carbide volume is broken into many smaller pieces distributed uniformly throughout the matrix, it becomes difficult for an abrasive to wear the matrix. Thus, the wear resistance increases. Wear resistance is defined as the ability for a material to resist material loss under an applied abrasive load. Ultimately an alloy's ability to protect the matrix and prevent cracking dictate the wear resistance of particulate reinforced alloys.

Along with size, the shape of a carbide effects the wear resistance of the bulk alloy. It has been show that below a hardness of 58 HRC, the bulk wear resistance is determined by the hardness of the carbides themselves[2]. Initially, the absence of alloying elements prevented

carbides from forming. Adding certain elements such as chromium and manganese allows carbides to form. However, these chromium and manganese carbides are relatively soft and even when present in high volume fractions, wear resistance eventually plateaus. Adding elements such as niobium, titanium and tungsten allow significantly harder carbides to form increasing the hardness and wear resistance. Once sufficient amounts of hard carbides form producing an increase in the bulk hardness to above 58 HRC, further increases in hardness do not directly correlate to increased wear resistance. At this point, the interplay between volume fraction of carbides and morphology becomes the mechanism of further alloy hardening and improved wear resistance. Rod-like or plate-like carbides have shown a susceptibility to cracking under load. Because of this, round carbides provide increased resistance to fracture and cracking thus leading to improved wear resistance. A factor yet to be controlled effectively is innate flaws in the carbides themselves. Carbides formed during alloy cooling contain defects such as voids and microcracks. These flaws provide stress concentrations and crack initiation sites. Due to the ceramic-like bonding, plastic deformation before fracture is limited or absent altogether. Reducing flaws in the carbides would reduce any stress concentrations resulting in an increase in wear resistance of the bulk alloy.

Many different classifications exist for carbides, however most carbides used in industrial applications fall into the interstitial carbide classification. These carbides are distinguished by their thermodynamic stability and high hardness. The name interstitial comes from where the carbon is located within the metallic lattice. Most carbides have a closed-packed crystal structure including face-centered cubic (FCC) and hexagonal close-packed (HCP). Although most carbides are close-packed, most of their host metals are not. The host metal is often body-centered cubic (BCC). These metals want to accommodate the carbon atoms in their lattice, so they form artificial close-packed structures. The carbon atoms also act to stabilize these

structures. In these lattices, there is an octahedral array of interstitial sites which carbon can occupy provided the ratio between host metal and carbon atomic radii is less than 0.59[3]. It is these interstitial carbon atoms which provide carbides with improved hardness over the host metal. If all of the interstitial sites are filled, a 1-1 stoichiometry is achieved creating a monocarbide which is denoted as MC where M stands for a combination of metallic elements totaling a stoichiometry of 1. However, it is also possible that not all of the sites fill with carbon. This is why many carbides in actuality form ratios of slightly less than 1 to 1.

Some of the most stable carbides are TiC, NbC and VC all roughly 1-1 stoichiometry. However, carbides can also have more than two metallic elements in their composition. These complex carbides can have, for example, niobium and vanadium bonded to the carbon. The complex niobium-vanadium carbide is denoted (Nb, V)C or MC where the M stands for a combination of transition metals. They can also take the form of M_2C, $M_{23}C_6$ and so forth. It is also possible for the interstitial element to contain both carbon and boron. This could be denoted as M(C,B) meaning both carbon and boron are present in a ratio that equates to a 1 to 1 stoichiometry with a metal. Some common and uncommon carbides in hardfacing alloys are listed in Table I.

Table I- Possible Carbides and Crystal Structures[4]

Carbide	ICDD	Structure	Lattice Parameters (nm)		
			a	*b*	*c*
Cr					
$M_{23}C_6$	5-721	FCC	1.06228		
$Cr_{23}C_6$	35-783	FCC	1.06599		
$(Cr,Fe)_7C_3$	5-720	Hexagonal	1.398		0.4523
Cr_7C_3	11-550	Hexagonal	1.398		0.4523
Cr_7C_3	36-1482	Orthorhombic	0.70149	1.2153	0.4532
Cr_3C_2	35-804	Orthorhombic	0.55273	1.14883	0.28286
Fe					
Fe_3C	34-0001	Orthorhombic	0.50915	0.67446	0.45276
Fe_3C	35-772	Orthorhombic	0.5091	0.67434	0.4526
Fe_7C_3	17-333	Hexagonal	0.6882		0.454
Fe_2C	36-1249	Hexagonal	0.2754		0.4349
Fe_2C	37-999	Orthorhombic	0.4704	0.4318	0.283
Nb					
NbC	38-1364	FCC	0.44698		
V					
V_8C_7	35-786	Cubic	0.833409		
W					
WC	25-1047	Hexagonal	0.29062		0.28378
W_2C	35-776	Hexagonal	0.2997		0.47279
$(W_4Ni_2)C$	20-796	FCC	1.125		
$(W_3Fe_3)C$	41-1351	FCC	1.11094		

In carbides, there is a complex combination of atomic bonding which greatly affects their stability and hardness. A mixture of ionic, covalent and metallic bonding provides varying degrees of stability and hardness[3]. Metal-metal and metal-carbon bonds combine to contribute to the total bond energy and thermodynamic stability (Table II).

Table II- Bond Types Contribute to Total Bond Energy, Correlating to Thermodynamic Stability[3]

Periodic Table Group	Metal-Metal Bond	Metal-Carbon Bond	Bond Energy (eV)	Melting Point of Carbide (^{0}C)
IV	Weak	Strongest	TiC → 14.66	TiC→3140
V	Stronger	Strongest	VC→13.75, NbC→16.32	VC→2810, NbC→3600
VI	Strongest	Weakest	Unknown	WC→2850, Cr_3C_2→2690

Table II shows that although Group IV elements have the strongest metal-carbon bonding, the metal-metal bond strength reduces the overall bond energy which lowers the melting temperature. When examining the Group V elements, NbC, has strong metal-metal and

metal-carbon bonds which produce the most thermodynamically stable carbide. The stability of carbides is due to a mixture of metal-metal and metal-carbon bonding. The metal-metal bond is straightforward and consists of a metallic bonding between two metallic atoms. The metal-carbon bond is more complicated consisting of both ionic and covalent components. The valence electrons for titanium (and all 4th row transition metals) consist of a partially filled 3d-orbital and a filled 4s-orbital[5]. These titanium orbitals interact with the 2p-orbital of carbon. In carbides consisting of titanium or niobium, there is a large electronegative difference between the metal and carbon. This allows for a strong ionic attraction. However, it has been suggested that the ionic component of titanium only accounts for 30% of the total metal-carbon bond[5]. The remaining 70% must be attributed to the covalent bond. Thus the strength, thermal stability and hardness of carbides can be attributed mainly to the covalent bonding. However, covalent bonding is highly directional with a specific bond direction providing the highest strength. Any deviation from this optimum orientation reduces the covalent strength. For example, the strongest carbides are titanium and niobium carbides. These carbides have roughly a 1-1 stoichiometry as a result of their NaCl crystal structure (Figure 2).

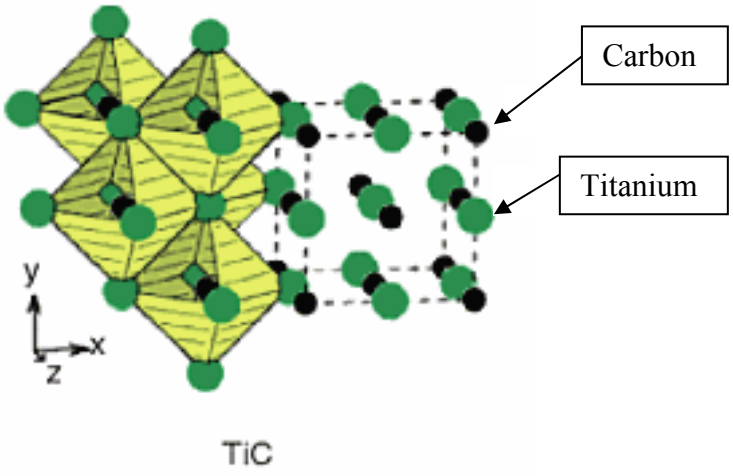

Figure 2-NaCl crystal structure of titanium carbide with carbon interstitials[6].

However, weaker carbides such as chromium carbide do not have a perfect NaCl crystal structure. They are metastable meaning that frequently chromium carbides have an irregular stoichiometry such as 3-1. The reason for this arises from the stability of the NaCl crystal structure. The presence and strength of carbon-carbon bonds effects the crystal structure stability. Titainum and niobium have a large difference in atomic radii compared to carbon meaning the separation between carbon atoms prevents significant interaction. However, as the metallic atoms decrease in size, a carbon-carbon bond develops and reduces the stability of the NaCl crystal structure and thus the carbide itself. The metastable nature of carbides similar to chromium carbide corresponds to a decrease in the covalent bond's strength.

The amount of carbon in an alloy can also cause negative effects on the wear resistance of an alloy. If too much carbon or boron is added relative to other carbide forming elements, not all the carbon can be used. As such, it will remain in solution with the austenite. This increases the hardenability of the matrix which can have detrimental effects. If martensite forms during the solidification process, large internal stresses are induced frequently producing weld-cracking. Cracking can be avoided by preventing any phase transformation from the austenite during solidification. There are few studies reporting the effect of boron on the wear resistance of hardfacing alloys; however, various studies support that boron does effect the wear resistance indirectly. By adding boron, austenite can be stabilized at lower temperatures[7]. However, retained austenite is metastable at normal operating temperatures. The advantage to this is that retained austenite easily transforms into martensite with energy input. During abrasive wear, heat is generated as a result of friction. This heat provides for a strain-induced phase transformation to martensite. This transformation has been shown to improve the wear resistance of hardfacing alloys[8]. The martensite is harder, providing the matrix with improved

wear resistance over ferrite or austenite alone. Also, the localized phase transformation minimizes internal strains which lead to cracking in bulk martensitic transformations.

Although most carbides form at higher temperatures directly from the melt, small amounts of carbon are held in solution within austenite, which becomes available upon transformation into ferrite at lower temperatures. This newly available carbon can bond with any carbide-forming elements not already tied-up in carbides. However, carbon is present in too low a percentage to form most carbides. The solution to this problem arises from the mechanism of austenite to ferrite transformation. The allotropic transformation occurs indirectly through the nucleation of ledges which grow laterally to the desired phase growth (Figure 3).

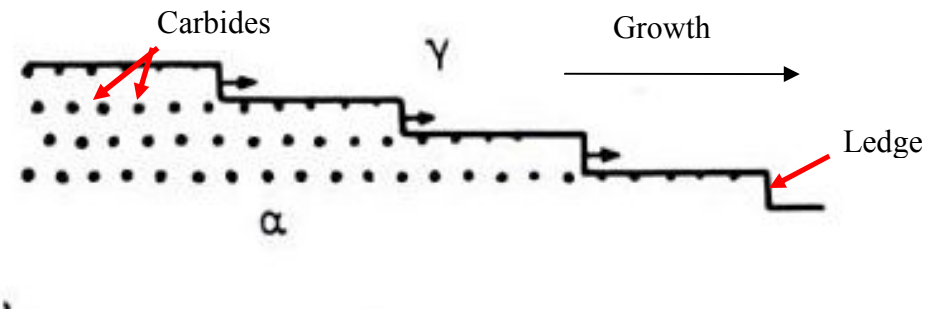

Figure 3-Ledges can be seen ratcheting across the α/γ interface leaving behind carbide precipitates[9].

As is depicted in Figure 3, ferrite ledges nucleate in the austenite and move across the austenite-ferrite boundary. As this occurs, a localized carbon supersaturation occurs until sufficient carbon is available to form a carbide. The ledge itself has higher energy as a result of incoherency with the austenite and would normally be the preferential nucleation site of carbides[5]. However, it is believed that the ledges move too rapidly to allow for nucleation and as a result, the carbides precipitate along the semi-coherent phase boundary. Thus, the carbides are coherent with the ferrite, however they must also be coherent with the austenite. A carbide will not precipitate unless the interfacial energy between matrix and carbide is sufficiently low[10]. In order for the ledge to not become pinned as a result of the carbide precipitation, the ledge height

must be sufficiently higher than carbide so it can pass over it. Once the ledge passes over a carbide imbedding it in ferrite, growth continues.

IV. Project Justification

In heavy industries such as oil drilling and ore mining, key components are exposed to harsh wear environments. Hardfacing is not a new development; it has been used extensively to provide a sacrificial layer over crucial components to prolong the operational life of a part . New alloys are constantly being investigated in the attempt to prolong the life of a part while retaining economic efficiency. It has been demonstrated in previous investigations from Scoperta that heavily alloying steel using niobium, vanadium and tungsten in total upwards of 30 wt% has the potential to reduce weld cracking while increasing the wear resistance over currently used alloys. By adding various alloying elements, the size and composition of complex carbides can be controlled leading to weldable, highly wear resistant alloys which can provide companies enhanced cost savings.

In most industries, time wasted equates to money wasted. When an oil drill bit dulls or fractures, time is spent repairing it. Similarly when the edge of a truck-mounted shovel dulls, efficiency is lost. By improving the wear resistance and weldability of a hardfacing alloy, the frequency of these costly repairs can be reduced. Reducing repairs leads to an increase in the profitability of a project. In mining and other earth-moving endeavors, the shovel used by front loaders has a hardfaced tip which is exposed to harsh conditions. By hardfacing, cost savings can quickly be realized. As Table III shows, the estimated savings as a result of hardfacing adds up to over $9000 per month for a front loader shovel.

Table III-Cost Savings Comparison Between Hardfaced and Non-hardfaced Front-loader Shovels

Equipment	Resulting Cost Increase from Hardface Per Shovel	Service Life Increase per Shovel (Hours)	Decrease in Used Shovels/Month	Savings ($)
Front-loader Shovel	150	200	-26.5	9100

The initial cost to hardface a shovel is $150 more than just the shovel. However, the service life of the shovel is longer than the non-hardfaced shovel. This means overall fewer shovels used which quickly outweighs the initial cost of hardfacing. This analysis does not include money saved by reducing downtime. If the shovel is running longer, more ore can be extracted and the profitability as a result of each shovel increases.

Procedure

I. Sample Preparation

The alloy samples were prepared by Justin Cheney at Scoperta Inc. using an arc-melt where weighed amounts of each elemental component were mixed together in a crucible and melted at roughly 4000^{o}C. Each alloy was cast into a roughly round shape. They were cut into roughly four equal quarter regions using a wet abrasive saw and mounted in Bakelite using a Buehler thermal mounting press. They were polished using standard metallography techniques.

In total, 13 alloys were prepared. An initial batch of seven alloys were cast where the total amount of C+B was constant at 3 wt%. The ratio of carbon to boron was varied where carbon was added and boron was removed (Figure 4).

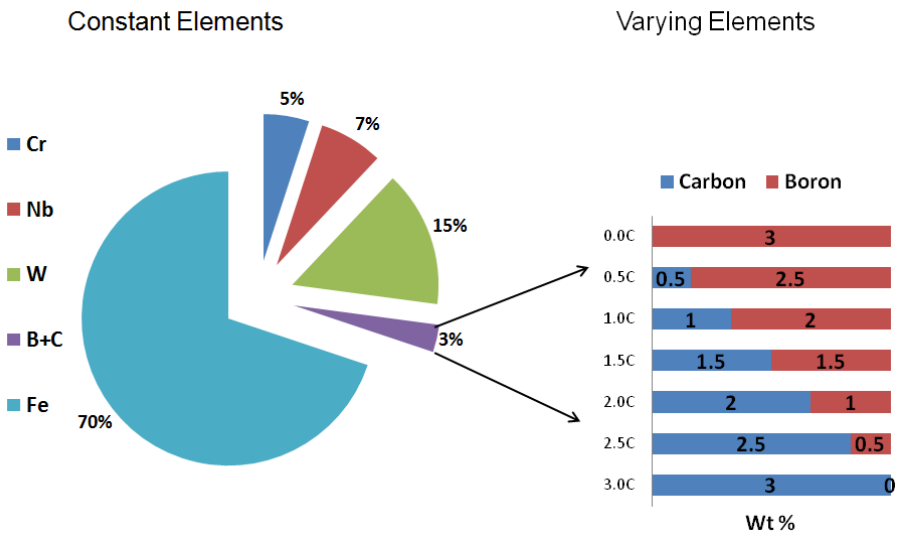

Figure 4- Weight percent compositions of the first seven alloys.

The second six samples were prepared using the same arc-melt process as before. For three samples, the amount of carbon and boron was held constant at 0.5 wt% and 2.5 wt%, respectively. However, tungsten was removed at intervals of 2 wt% per sample and replaced with vanadium in an equal amount (Table IV).

Table IV-Weight Percent Compositions of Second Six Alloys

Sample	Fe	Cr	Nb	V	B	C	W	Si	Ti	B+C
First round sample	69.6	5	7	0	2.5	0.5	15	0.15	0.25	3
1	69.6	5	7	2	2.5	0.5	13	0.15	0.25	3
2	69.6	5	7	4	2.5	0.5	11	0.15	0.25	3
3	69.6	5	7	6	2.5	0.5	9	0.15	0.25	3
4	69.85	5	7	0	2.5	0.25	15	0.15	0.25	2.75
5	69.85	5	7	0	2.25	0.5	15	0.15	0.25	2.75
6	70.1	5	7	0	2	0.5	15	0.15	0.25	2.5

Rather than testing an alloy again, the first round alloy with 0.5 wt% C was used as the alloy without any vanadium as shown in Table IV.

II. Hardness

Each of the mounted samples was hardness tested using a microhardness tester. Each sample was tested in 10 random locations. The reported values were taken as the average of all tests performed on each sample. In addition, on samples where the microstructure appeared non-uniform, a hardness profile was performed taking readings every 10 μm.

III. Scanning Electron Microscope and Energy Dispersive Spectroscopy

Each of the samples was left in the Bakelite mount and electrically grounded to a SEM sample stem using copper tape. Each sample was imaged in high vacuum using a backscatter detector in order to better distinguish between phases.

To determine the compositions of the phases, EDS was used. For each phase in each alloy, the composition was measured at three different locations. These values were averaged for the reported values stated in the Results. The electron beam was run at 20 keV roughly doubling the alloying element with the largest Kα.

IV. X-ray Diffraction

One scan was performed per alloy in order to determine the crystal structure of the present phases. A Cu-Kα source was utilized for the x-rays. The polished samples were broken out of their Bakelite mounts and placed on a sample holder using non-crystalline clay to hold the samples in place. The scan increment was 0.04 degrees with a scan speed of 8 seconds per increment. Using a scan range of 20-120 degrees, the total scan time was 9.5 hours.

V. Volume Fraction Measurements

The carbide and matrix phases volume fractions were measured utilizing IQ Materials image analysis software analyzing high contrast images taken using backscatter electrons. The range of intensities was manually adjusted so that each intensity region covered only one phase. Care was taken to insure no intensities overlapped, otherwise inaccurate measurements would

have occurred. This measurement process was performed for each alloy using 3 images at three different magnifications. The individual volume fraction results were averaged.

VI. Wear Testing

To test the relative wear resistance of the alloys, a rotary wear tester was fabricated. Using a variable speed rotary metallographic polishing wheel, 60 grit sand paper was placed on the wheel. 60 grit sand paper corresponds to a average particle size of 250 μm. Then an arm was fabricated out of wood in order to hold the samples steady and at fixed locations. This arm was then attached perpendicular to another piece of wood and clamped to the work bench using a c-clamp. Lead shot was weighed at 685 g and set in a cup located directly over the test sample to apply a constant load. Each sample was run for 10 minutes then moved to another radial location on the sandpaper to expose the sample to fresh abrasion not worn down by previous testing (Table V).

Table V-Radial Distance and the Time of Wear Testing

Sample Time (min)	Radial Distance (in)
10	7.50
20	6.75
30	6.25

To insure consistent locations of the sample on the polishing wheel, markers were made on the table. The support structure was slid back, corresponding to a decrease in distance which the sample was from the center of the wheel (Figure 5).

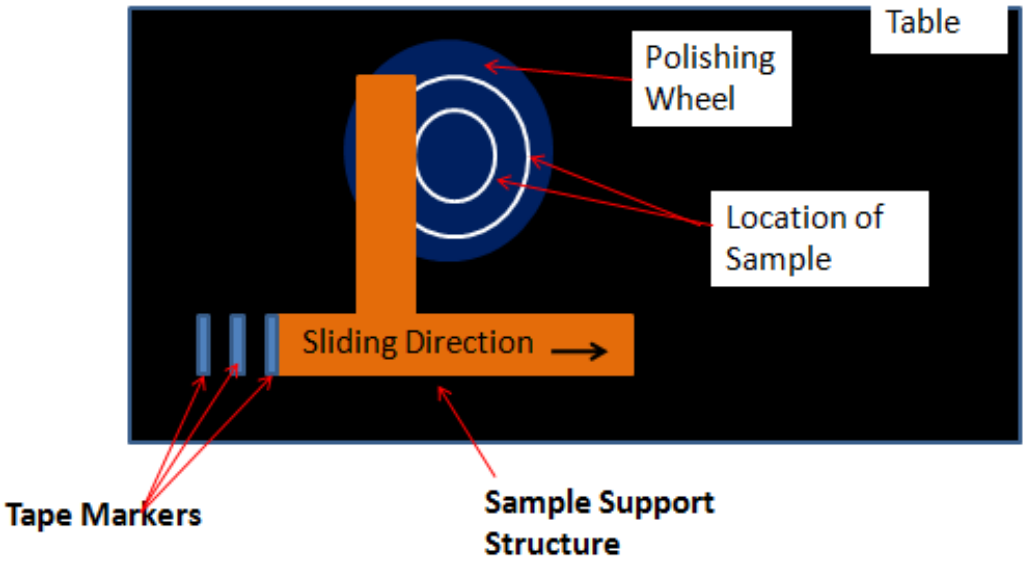

Figure 5-Diagram illustrating how as the structure was slid, the radial distance of the sample decreased.

Results

I. Microstructural Analysis

Based with Scoperta, it was expected that variations in the carbide/boride type as well as the amount of a carbide would have a significant effect on an alloy's wear resistance. As such, microstructural analysis was performed to identify potentially promising alloys. The first round of alloys demonstrated a microstructural evolution as carbon was added. With the 0.0 wt% C sample, there were only two phases present. The cubic boride phase distributed in a matrix of ferrite (Figure 6).

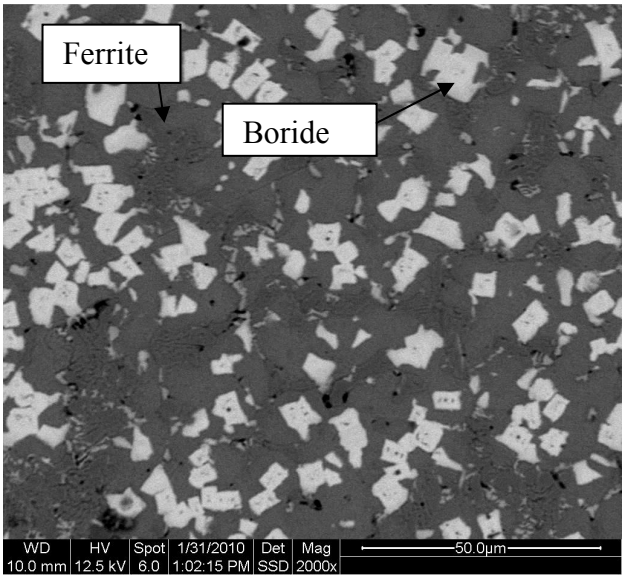

Figure 6- BSE image of the 0.0 wt% C alloy. The borides are segmented rather than a continuous phase.

As carbon was added, the cuboidal phase became NbC while a second carbide rich in tungsten formed. This second carbide surrounded the NbC and emanated away in a lemellar pattern (Figure 7).

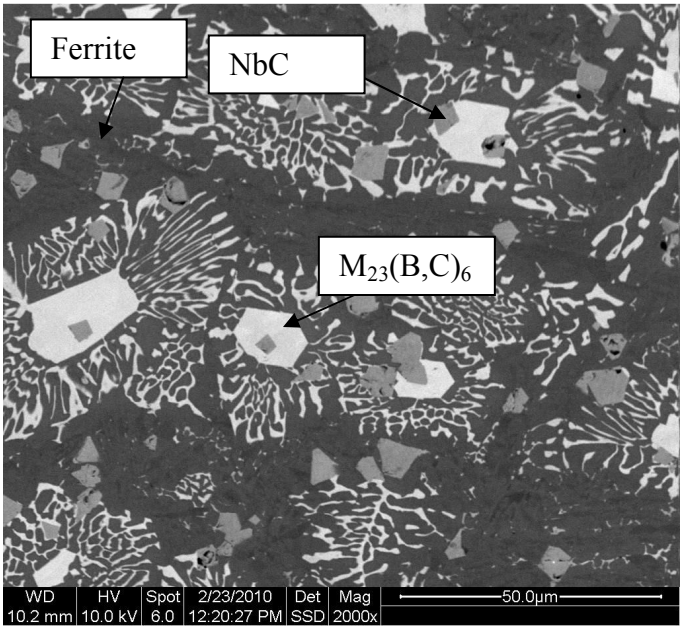

Figure 7-BSE image of 0.5 wt% C alloy. Increased carbon content allows for nucleation of the $M_{23}(B,C)_6$ carbide.

As can be seen in Figure 7, the NbC is cuboidal, suggesting coherency with the ferrite matrix. However, both the NbC and the tungsten-rich carbide are evenly distributed throughout the ferrite matrix. The tungsten-rich carbide, through EDS and XRD analysis was shown to likely be a $M_{23}(C,B)_6$ carbide. Whether or not it is indeed the $M_{23}(C,B)_6$ carbide, it will be referred as such for identification purposes. The combination of hard carbides along with a relatively large amount of ferrite showed promise for weldability as well as wear resistance. It can also be seen that all of the $M_{23}(C,B)_6$ carbide grew from NbC. This suggests that the NbC served as a nucleation site for the $M_{23}(C,B)_6$ carbide.

Further increasing the carbon content produced a third Fe-rich carbide (Figure 8). Again, this carbide could not be definitively identified, however will be referred to as $M_{2,3}C$. Generally, as the amount of carbon increased, so did the amount of this third Fe-C carbide while there was a corresponding decrease in the amount of $M_{23}(C,B)_6$.

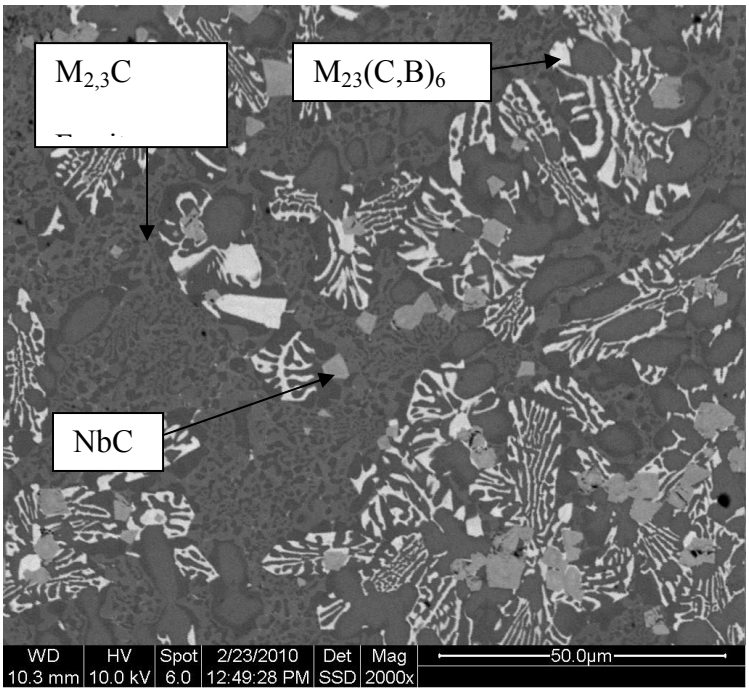

Figure 8- BSE image of 1.0 wt% C alloy. The matrix consists of a large volume of ferrite and the $M_{2,3}C$ carbide.

For the 3.0 wt% C sample, there was an apparent dendritic structure. In the interdendritic region, a lamellar distribution of what appeared to be two carbide phases nucleated. $M_{2,3}C$ carbide was the large volume white carbide, and an unidentifiable second carbide was located in between. However, still present in a large amount was the NbC (Figure 9).

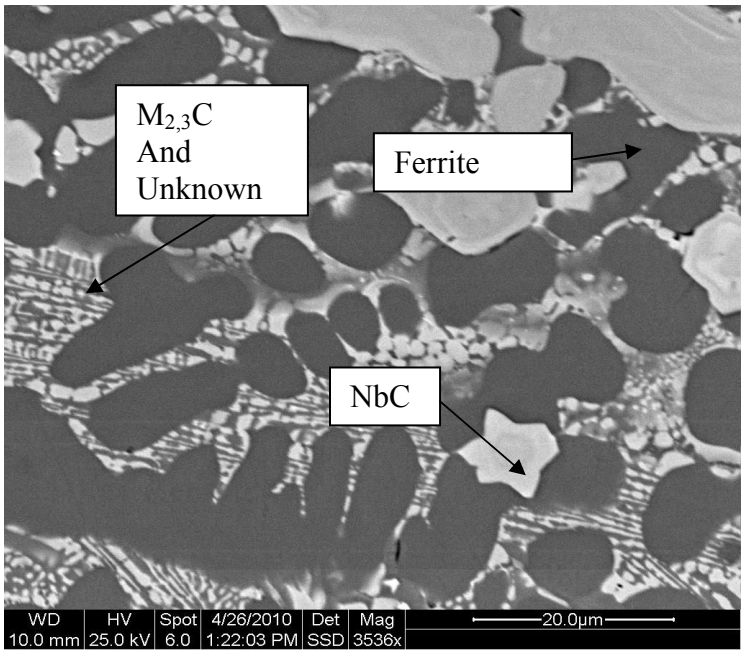

Figure 9- BSE image of 3.0 wt% C alloy showing a lamellar phase in the interdendritic regions.

The second alloy set developed from the first where the 0.5 wt% C alloys was a baseline. Adding vanadium to the 0.5 wt% C alloy refined the size of the niobium carbides while also segmenting the third carbide phase. This third carbide was no longer continuous and many smaller carbides nucleated instead. None of these smaller carbides could be identified with equipment available at Cal Poly (Figure 10).

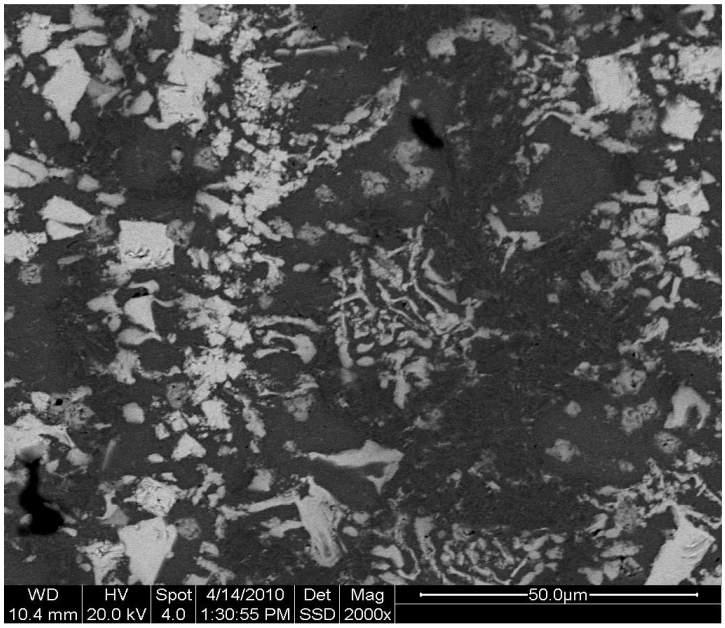

Figure 10- BSE image of alloy sample #1 from the second alloy set. This representative microstructure shows the addition of vanadium prevented large, continuous carbides from forming.

Although the second alloy set had sufficient ductile ferrite, there was a reduction in the amount of carbide suggesting an inability to prevent wear. The reduced carbide particle size also increases the possibility of spalling occurring under abrasive wear.

II. Relationship Between Carbon and the Volume Fraction of Each Carbide Phase

Through increasing carbon contents, the first round alloys developed various amounts of each phase. The reduction in the amount of one carbide had to be replaced by another carbide. However, increasing the carbon content showed no correlation with the volume fraction of any of the carbides (Figure 11).

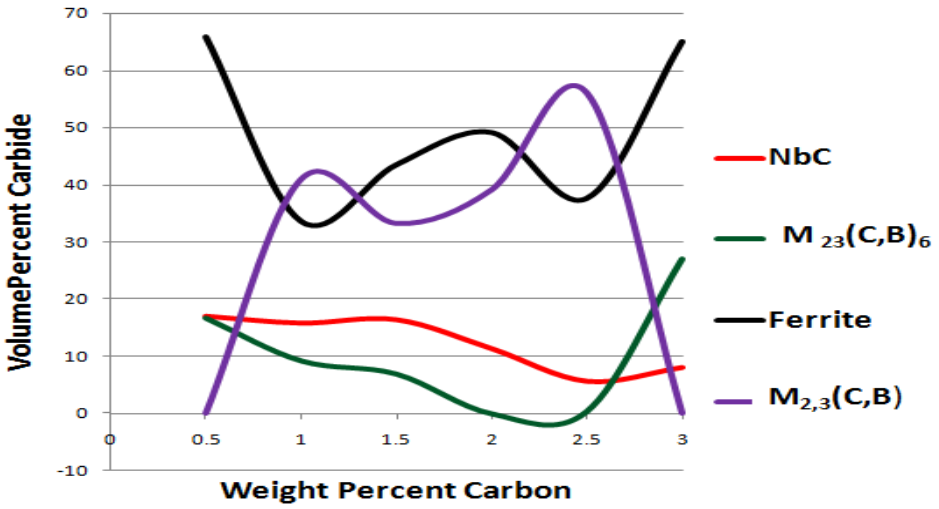

Figure 11- The effect of carbon content on the volume fraction of each phase in the first round alloys.

Determining the phases in each alloy showed a M_2C and M_3C carbide which are located in similar locations in the microstructure and have similar compositions. It was decided that because of the similarities between the two carbides, the were analyzed as one carbide ($M_{2,3}C$). As can be seen, a reduction in $M_{2,3}C$ results in a equal increases in the volume of ferrite. The high concentration of Fe in the $M_{2,3}C$ carbide explains why the amount of ferrite is inversely related. There is insufficient amounts of Fe for both ferrite and $M_{2,3}C$ to be present in equal amounts. Also, NbC remained relatively constant regardless of carbon content demonstrating the volume fraction is determined by the amount of Nb, which was constant, and not the amount of carbon. The $M_{23}(C,B)_6$ carbide decreased until it was absent in the 2.0 wt%C and 2.5 wt% C alloys. No explanation could be determined and a continuation of this study would likely involve investigating the behavior of the $M_{23}(C,B)_6$ carbide.

III. Phase Composition Analysis

EDS provided relative amounts of each alloying element present in each phase. Exact compositions of each phase could not be determined due to the inability to measure the presence of carbon. The small atomic mass of carbon prevents its detection thus it was ignored when

calculating the atomic percents. The exact measured compositions were not reported, suffice to say they when compared to XRD results, they supported the presence of the carbides reported previously.

IV. Hardness

It was expected that an increase in carbon content would increase the hardness of the alloy, however this was not the case. Varying the carbon content of each alloy resulted in varying carbide volume fractions, but, no single carbide controlled that alloy hardness alone. The factor most affecting the hardness was the combined volume fraction of carbides. As the total amount increased, so did the hardness (Figure 12, Table VI).

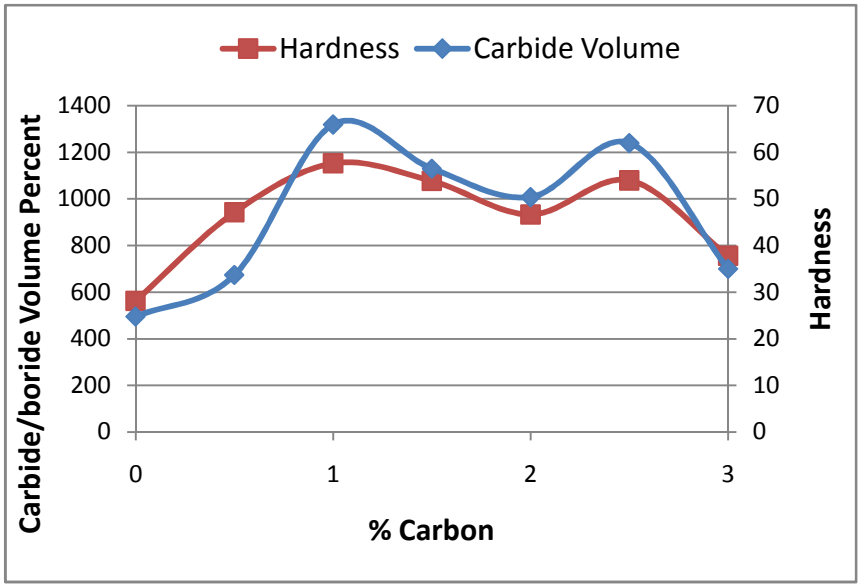

Figure 12- Relationship between hardness and total volume percent carbide for first round alloys.

Table VI- 1st Round Alloy Set Hardness

Sample	Average Hardness (HV)
0.0 wt% C	563.2
0.5wt% C	942.8
1.0wt% C	1152.6
1.5wt% C	1077.6
2.0wt% C	933.4
2.5wt% C	1079.4
3.0wt% C	756.2

As can be seen, the highest hardness was seen at 1 wt% carbon where there was 66 % carbide while the lowest hardness in the initial set of alloys was seen at 0.0 wt% C where there was 24% boride reinforcement.

The second set of alloys based on the original 0.5 wt% C alloy were also hardness tested. All seven alloys showed a lower hardness than the first round of alloys while also failing to meet the minimum hardness of 830 HV (Table VII).

Table VII- Hardness of the Second Alloy Set

Alloy	Average Hardness (HV)
1	639
2	429
3	293
4	660
5	715
6	693

Based on this data and the inability to obtain further results from the other analysis techniques, the second round alloys were determined to show insufficient potential to warrant further testing.

V. X-ray Diffraction

XRD enabled the determination of the crystallographic structure with mixed results. In each sample, it was determined that there was ferrite as well and NbC with a 1-1 stoichiometry. However, the database limitations prevented definitive identification of the other two carbide phases (Figure 13).

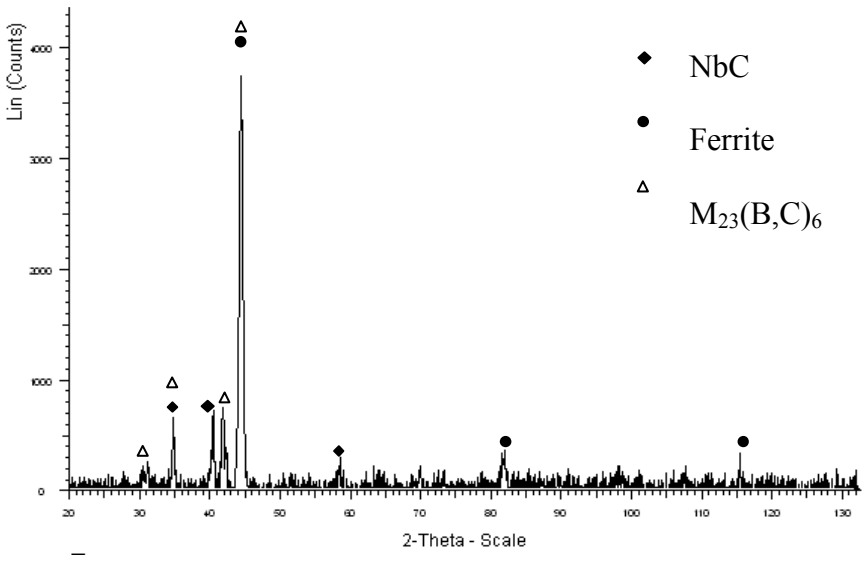

Figure 13- XRD scan of the 0.5wt% C sample. Similarity between carbide spectrums prevents definitive identification.

There appears to be a close match with $M_{23}(B,C)_6$. Examining the EDS results as well, the composition of the second carbide/boride phase further suggests a $M_{23}(B,C)_6$. The database used did not list this carbide, however literature suggests this phase is likely the $M_{23}(B,C)_6$ carbide. As further increases in carbon content continue, a third carbide/boride develops whose spectrum suggests M_3C or M_2C depending on the alloy (Figure 14).

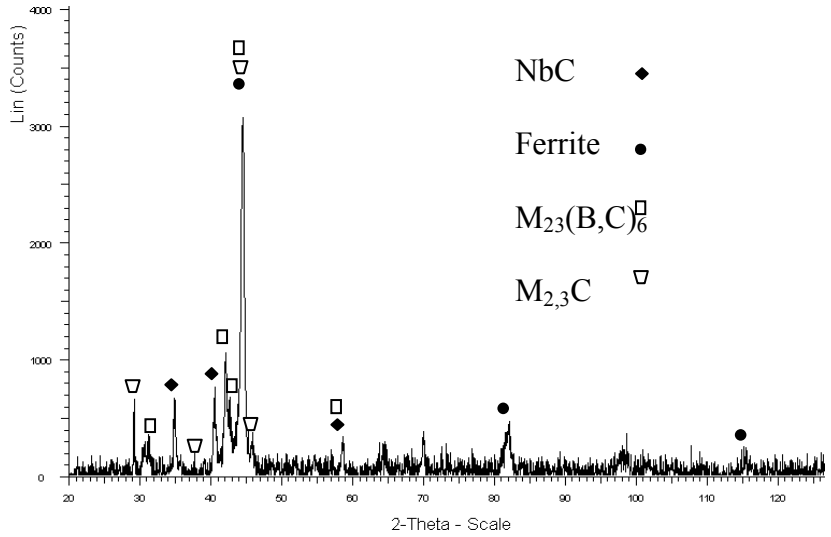

Figure 14- XRD scan of 1.0 wt% C sample. This spectrum is representative of the alloys up to 2.5 wt% C where the M_2C or M_3C are exclusively present in various alloys. Both are never present together.

Further increasing carbon to 3 wt% shows disappearance of the $M_{23}(B,C)_6$ phase completely with only NbC and $M_{2,3}C$ remaining (Figure 15).

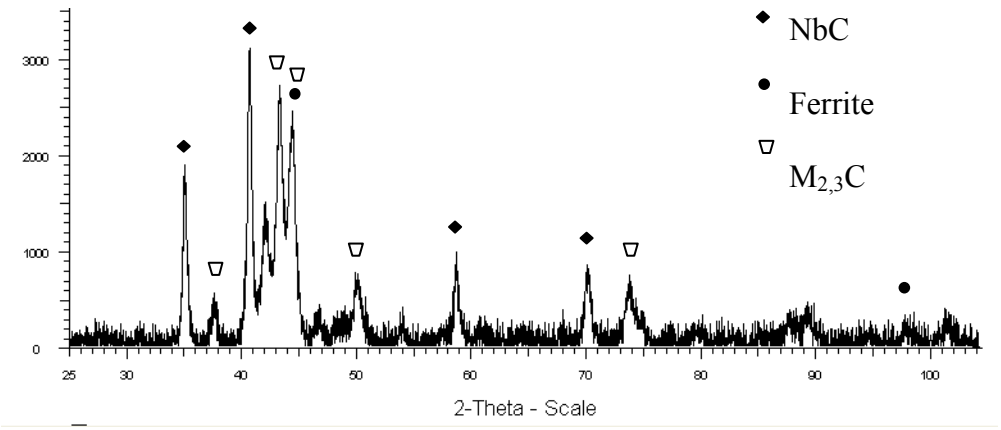

Figure 15- XRD scan of 3.0 wt% C sample. The unidentified peaks could not be matched to any carbide in Cal Poly's database.

VI. Wear Resistance

Using a custom wear tester, the relative wear resistance of the first alloy set was tested. These results are not quantitative and provide only comparative wear resistance measurements. It was seen that there was a correlation between the hardness and the mass loss of material (Figure 16, Table VIII).

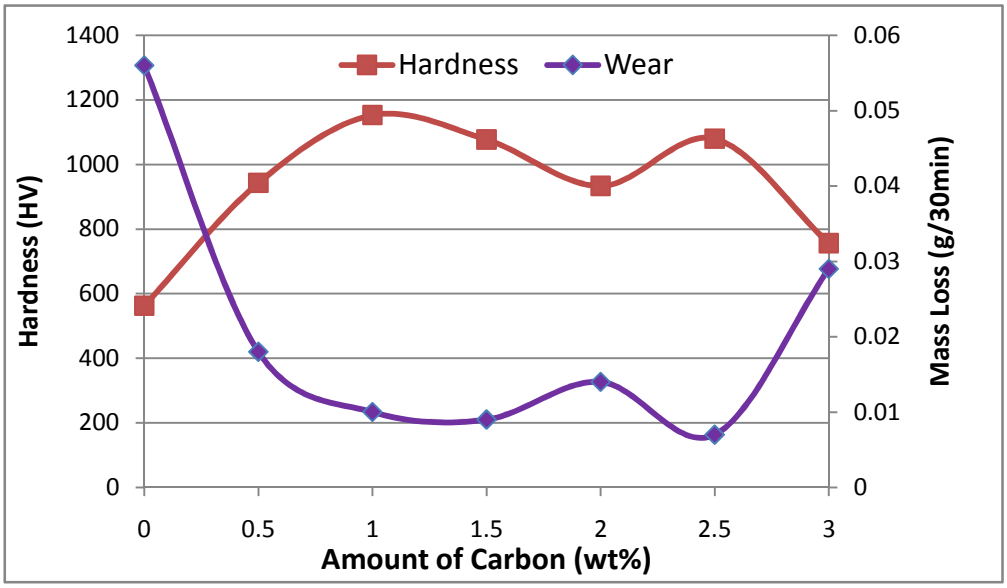

Figure 16-The relationship between hardness and mass loss from wear testing.

Table VIII- Mass Loss After Wear Testing for 30 Minutes

Alloy	Mass Loss (g)
3.0 wt% C	0.029
2.5 wt% C	0.007
2.0 wt% C	0.014
1.5 wt% C	0.009
1.0 wt% C	0.01
0.5 wt% C	0.018
0.0 wt% C	0.056

As can be seen in Figure 16, the lowest hardness had the highest mass loss while the highest hardness had the least material loss.

Discussion

I. Evolution of Carbides and Their Effects on Solidification

It can be noticed in all the alloys that a niobium rich phase nucleates as either a carbide or boride. This is likely due to the high thermal stability of NbC with a melting temperature of 3610^{o}C[11]. When the alloy ingots were cast, NbC was the first phase to form directly in the melt. This is demonstrated by the cuboidal shape of the carbide. NbC was able to nucleate in its natural shape as dictated by the cubic crystal structure. It was also noticed that the volume fraction of NbC was constant regardless of carbon or boron content. Niobium has a high reactivity, exceeded only by titanium. At high temperatures, niobium has little thermodynamic competition to form a carbide, thus it becomes saturated with carbon. Extra carbon has no effect on the NbC volume.

Looking at the 0.5 wt% C alloy, the $M_{23}(C,B)_6$ carbide it nucleates around the NbC, in many cases encasing the NbC completely. It is likely that the $M_{23}(C,B)_6$ forms from the melt as well and prevents coalescence of the NbC into larger particles. The $M_{23}(C,B)_6$ carbide has insufficient driving force to homogeneously nucleate at the higher temperature in the melt.

However, the NbC provides heterogeneous nucleation sites effectively lowering the critical nucleation radius of the carbide (Figure 17).

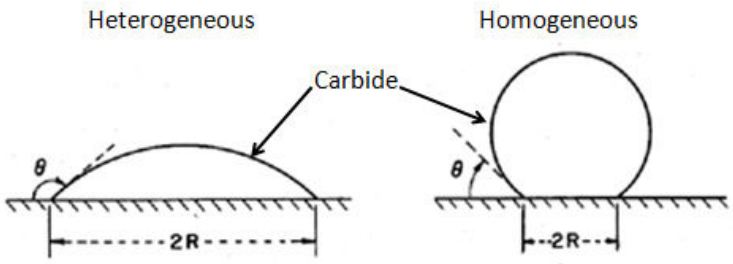

Figure 17- Comparison of heterogeneous and homogeneous nucleation of a carbide.

If the assumption is made that the carbide precipitates in a cuboidal shape, the critical radius of nucleation is defined by Equation 1.

$$r^* = \frac{-4\gamma}{\Delta G_v} \qquad (1)$$

Equation 1 states that r* is dependant on the surface energy required to nucleate and the volumetric free energy. When the wetting angle increases, the effective ΔG_v decreases, requiring less undercooling to achieve the critical nucleation radius. After nucleating around the NbC carbide, $M_{23}(C,B)_6$ continues to grow in a lamellar orientation with ferrite inbetween carbide rods radiating outwards.

When examining the alloys with greater than 0.5 wt% C, a dendritic configuration of the ferrite occurs. As solidification procedes, the austenite has a carbon saturation less than the total carbon in the alloy. To accomadate this, the carbon is ejected into the region in between dendrites (Figure 18).

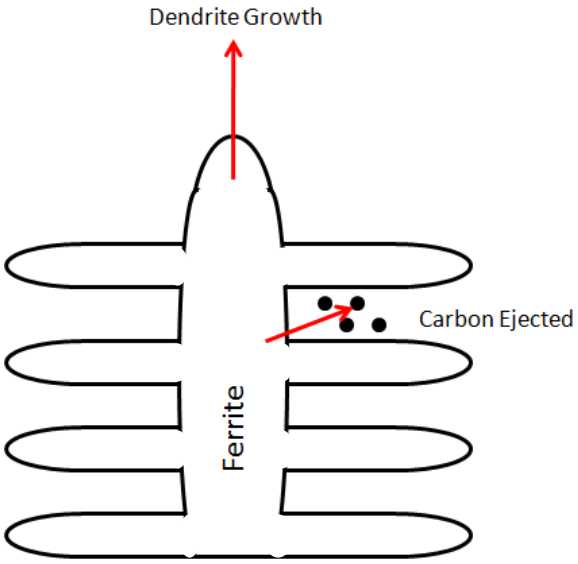

Figure 18- Ferrite dendritic growth as carbon is ejected into the interdendritic region.

In these interdendritic regions, a carbon concentration develops. When sufficiently high, the $M_{2,3}C$ phase nucleates at elevated temperatures. When austenite becomes unstable at 727°C, rather than nucleating Fe_3C as dictated by equilibrium thermodynamics, the newly available carbon forms the $M_{2,3}C$ carbide.

II. Carbide Evolution

It was observed that at carbon contents above 0.5 wt% C, the $M_{2,3}C$ carbide nucleated. This carbide developed as a result of excess carbon in the alloy. Below 1.0 wt% C, all the carbon formed $M_{23}(C,B)_6$ and NbC. At lower carbon concentrations, the boron acted to stabilize the $M_{23}(C,B)_6$ carbide as demonstrated by the greater volume fraction of the carbide. As the carbon content increased, the volume fraction decreased.

It is not clear whether this phase has only carbon bonding in the carbide, or if a more accurate carbide stoichiometry is $M_{23}(C,B)_6$ where boron takes part in atomic bonding. It was been shown that boron acts to stabilize carbides explaining why the volume fraction of $M_{23}(C,B)_6$ was lower at lower carbon contents (thus higher boron contents). As the amount of

carbon increased and the boron decreased, the carbide coarsened and grew larger in total volume. Eventually, with the absence of boron in the 3.0 wt% C alloy, the $M_{23}(C,B)_6$ completely destabilized, becoming

It was also noticed through EDS that a measurable amount of about 2.5 wt% Ti was seen in the NbC carbide in every alloy. This at first might seem like a irregular reading. However, it can be explained through the thermodynamics of Ti and carbon. Ti has the strongest carbide forming tendencies exceeding those of niobium. In these alloys, there are insufficient amounts of Ti to form their own carbides, however when NbC forms, Ti is attracted to the carbide. Titanium does not take part in atomic bonding, however it becomes centralized at the NbC carbides. Thus even at an overall alloy concentration of 0.1 wt%, Ti becomes measureable.

III. Microstructure Effects Wear

With the limited wear testing performed, it was shown that the alloy hardness directly controlled the wear resistance of the first round alloys. This in turn means that the wear resistance was determined by the total volume fraction of carbides. Although previous literature suggests that carbide morphology has the greatest effect on wear, its effect on the alloys tested in this study was insignificant.

Although this study showed carbide volume fraction controlled wear resistance, further testing would likely show the effect of carbide morphology on wear resistance. The $M_{23}(C,B)_6$ carbide which has shown the most promise of improving wear resistance in previous studies is hard, however more ductile than either the NbC or the $M_{2,3}C$ phase (Figure 19).

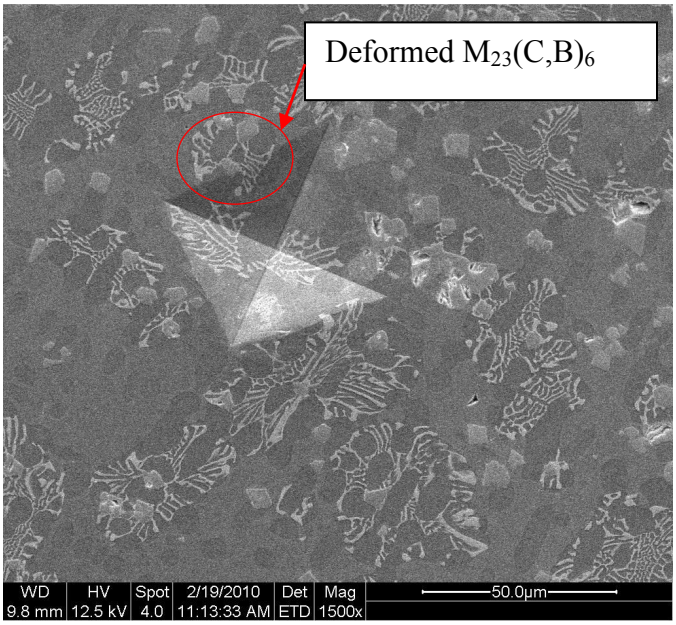

Figure 19- BSE image of a microhardness indent showing deformation of the lamellar $M_{23}(C,B)_6$ carbide

Rather than breaking when a load was applied, the lamellar carbide mearly deformed. This has been shown to improve wear resistance through prevention of spalling. When carbides crack, it becomes easier for segments of them to spall out of the ferrite. Carbides able to bend under an applied load can continue to protect the matrix while also retaining the strength of their phase boundary. This increased interfacial strength is a result of increased surface area of the $M_{23}(C,B)_6$ carbide. This has been shown in previous studies to reduce the wear resistance and supports the promise of the wear resistance of the 0.5 wt% alloy[12].

Conclusions

1. The 0.5 wt% carbon alloy has the greatest potential for wear resistance while also likely retaining weldability.
2. Total carbide volume fraction was the major factor affecting the hardness of the alloys. Increasing carbide volume fraction increased the hardness.
3. Adding vanadium to the 0.5 wt% C alloy showed little promise of wear resistance being softer and having a broken carbide microstructure.
4. Initial wear testing showed the 0.5 wt% C alloy had a mass loss similar to that of the higher carbide volume fraction alloys at 0.018 g/30 min.

References

[1] "Welding." *Mig Industrial Engineering*. Web. 02 June 2010. <http://www.migindustrialengineering.com.au/welding.html>.

[2] Wei, Shizhong Wei, Jinhua Zhu, and Leuju Xu. "Research on wear resistance of high speed steel with high vanadium content." *Materials Science and Engineering: A* 404.1-2 (2005): 138-45. Print.

[3] Pierson, Hugh O. Handbook of refractory carbides and nitrides properties, characteristics, processing, and applications. Park Ridge, N.J: Noyes Publications, 1996. Print.

[4] Hetzner, Dennis W., and William Van Geertruyden. "Crystallography and Metallography of Carbides in High Alloy Steels." *Materials Characterization* 59 (2008): 825-41. Print.

[5] Zhang, Yongfan, Lixin Zhou, and Shengchang Xiang. "A Theoretical Study on the Chemical Bonding of 3d-transition-metal Carbides." *Solid State Communications* 121.8 (2002): 411-16. Print.

[6] "Hafnium." *Periodic Table of Elements and Chemistry*. Web. 03 June 2010. <http://www.chemicool.com/elements/nacl.html>.

[7] Kim, Ji, Kang Ko, Gyung Kim, and Seung Noh. "The effect of boron on the abrasive wear behavior of austenitic Fe-based hardfacing alloys." *Wear* 267.9-10 (2009): 1415-419. Print.

[8] Lee, K., S. Lee, Y. Kim, and H. Hong. "The Effects of Additive Elements on the Sliding Wear Behaivor of Fe-based Hardfacing Aloys." *Wear* 255 (2003): 481-88. Print.

[9] Durand-Charre, Madeleine. *Microstructure of Steels and Cast Irons*. Vol. 1. Heidelberg: Springer, 2004. Print.

[10] Fang, Hong-Sheng, Jia-Jun Wang, and Yan-Kang Zheng. "Formation mechanism of bainitic ferrite and carbide." *Metallurgical and Materials Transactions A* 25.9 (1994): 2001-007. Print.

[11] Shi, Liang, Yunle Gu, Luyang Chen, and Zeheng Yang. "Synthesis and Oxidation Behavior of Nanocrystalline Niobium Carbide." *Solid State Ionics* 176 (2005): 841-43. Print.

[12] Chatterjee, S., and T. Pal. "Wear Behaviour of Hardfacing Deposits on Cast Iron." *Wear* 225 (2003): 417-425. Print.